

HIGH CURRENT BEAM DYNAMICS SIMULATION IN THE PROTON STORAGE RING
 V.A.Moiseev, P.N.Ostromov
 Institute for Nuclear Research of the Academy of Sciences of the USSR
 Moscow 117312, USSR

Summary

The proton storage ring is intended to transform the time structure of the accelerated beam of the INR meson facility [1]. The 600 MeV H⁻ beam after the linac will consist of the sequence of 100μs pulses with 100Hz repetition rate and 50mA peak current. The H⁻→H⁺ charge-stripping injection will be used for accumulation entire linac macropulse (3·10¹³ particles).

There are two main modes of the storage ring operation.

1. Slow extraction mode (SEM) :
 tunes $\nu_x=1.85, \nu_y=1.90$
 stored beam emittances $\epsilon_x=1.5 \pi \cdot \text{cm} \cdot \text{mrad}, \epsilon_y=6.0 \pi \cdot \text{cm} \cdot \text{mrad}$
 filling time 100 μs
 extraction time ~ 9.9 ms
2. Fast extraction mode (FEM) :
 tunes $\nu_x=2.4, \nu_y=2.3$
 stored beam emittances $\epsilon_x=3.0 \pi \cdot \text{cm} \cdot \text{mrad}, \epsilon_y=3.0 \pi \cdot \text{cm} \cdot \text{mrad}$
 filling time 100 μs
 extraction time ~ 430 ns

In both modes the high stored current (~11.3A) and low energy ($\gamma=1.64$) result in a strong space charge influence displayed in the tune spread, transverse emittance growth, particle redistributions in real and phase spaces.

This paper summarizes the results of investigation of these effects for the INR proton storage ring using the macroparticle computer model [2].

Simulation algorithm

In the mathematical model we consider only transverse beam dynamics because the special azimuth filling [1] results in the negligibly small longitudinal component of the intrinsic field. Therefore the simulation algorithm consists of the next procedures.

1. Calculation of the space charge density $\rho(\vec{r})$ in the mesh points on the base of the known (set or calculated) macroparticle distribution function.
2. Determination of the electric field $\vec{E}(\vec{r})$ at the mesh points by solving the grid Poisson equation

$$\frac{1}{r} \frac{\partial}{\partial r} \left[r \frac{\partial \psi(r, \theta)}{\partial r} \right] + \frac{1}{r^2} \frac{\partial^2 \psi(r, \theta)}{\partial \theta^2} = - \frac{\rho(r, \theta)}{\epsilon_0} \quad (1)$$

with the following boundary conditions:

$\psi(R, \theta) = 0; \psi(r, \theta) = \psi(r, \theta + 2\pi l)$, where l is integer. The effective computation method [3] has been used to solve equation (1) on a regular mesh. The solution is determined on the grid (r_k, θ_n) in the form

$$\psi(r_k, \theta_n) = \sum_{i=0}^{N_\theta/2} [R_i(r_k) \cos(i \cdot \theta_n) + Q_i(r_k) \sin(i \cdot \theta_n)] \quad (2)$$

where $R_i(r_k), Q_i(r_k)$ are cubic splines,
 $\theta_n = n \cdot \Delta\theta, n = 0, (N_\theta - 1), \Delta\theta = 2\pi / N_\theta;$
 $r_k = k \cdot \Delta r, k = 1, N_r, \Delta r = R / N_r;$ (3)
 N_θ, N_r are integer.

The computation algorithm for finding the potential (2) consists of the fast Fourier analysis of the right side of equation (1) over the angular variable, the solutions of the linear equation systems for the spline coefficients and the fast Fourier synthesis.

3. Calculation of intrinsic beam magnetic field on the grid (3) by particle-grid technique.
4. Integration of the macroparticle motion equations in an external and intrinsic electromagnetic fields.

5. Accuracy check. It has been based on the energy conservation of the transverse motion connected with space charge field. During 1000 turns (the accumulation is completed after 227 turns) the energy fluctuation did not exceed 2%.

Betatron tune calculation

Usually the incoherent tune shift of the high intensity beam is calculated using the smooth approximation [4]. But this is only qualitative estimation for location of the working point on the betatron tune diagram. More perfect information about the space charge influence on the betatron tunes may be obtained by calculation of the betatron tune spread. The particle image in the (w, v) phase space, where $w = u / \sqrt{\beta_u}, v = (\alpha_u \cdot u' + \beta_u \cdot u) / \sqrt{\beta_u}$, u is either x or y, α_u and β_u are Twiss parameters at the fixed azimuth, will lie on the circumference. The change in particle location will be $2\pi \cdot \nu_u$ after one turn. Hence we can define ν_u . Making this procedure for all particles we can obtain the betatron spectrum on the turn.

Injection

The expected emittance of the injected H⁻ beam is $0.3 \pi \cdot \text{cm} \cdot \text{mrad}$ at the 3σ level that is essentially less than the emittances of a stored beam. This enables to use a charge-exchange multiturn spiral injection to reduce the passes of circulating protons through the stripping target and to fill both phase planes more uniformly [5]. We assume that the equilibrium orbit of stored beam at the azimuth of the stripping foil and vertical coordinate of injected beam on the stripping foil are moved in proportion of the injection time. It was shown [5] that a number of proton passes through the foil is reduced essentially by using spiral injection. Therefore the foil's heat load is decreased, its lifetime is increased and the influence of the multiple scattering on the stored beam quality is reduced.

Fast extraction mode simulation

The characteristic functions of one half ring period are shown in fig.1 for a isochronous regime. The r.m.s. emittance ϵ_{rms} , the effective emittance ϵ (more than 98% of stored particles), betatron tunes and average of passes of the stripping foil per stored proton are presented in Table 1 after the injection completion. The results of simulation display: a) the distributions in xx' and yy' phase spaces are almost homogeneous after the injection completion, r.m.s. emittances are not differed essentially from effective emittances; b) space charge leads to decrease of $\epsilon_{x rms}$ and increase of $\epsilon_{y rms}$ during injection; c) space charge causes essential increase of ϵ_x (~26%) and slight growth of ϵ_y (~6%).

The betatron spectra after injection completion are shown in fig.2. Detailed analysis shown that only particle injected at the beginning are in the resonance band $4\nu_y = 9$ and their perturbed phase trajectories lie inside beam phase volume yy' . Therefore Coulomb force nonlinearity leads to slight growth of ϵ_y . In the resonance band $3\nu_x = 7$ after the injection completion there are about 14% of stored particles lying in the periphery of the beam xx' phase space. The increasing of betatron oscillation amplitude of these particles leads

TABLE 1

Parameters	Fast extraction mode				Slow extraction mode					
	Without space charge		With space charge		Without space charge		With space charge			
	x	y	x	y	x	y	Injection		1000 turns	
							x	y	x	y
$4\epsilon_{rms}$, π -cm.mrad	2.24	2.24	2.21	2.35	0.94	4.75	0.99	3.85	1.19	3.90
ϵ , π -cm.mrad	2.76	2.85	3.48	3.03	1.39	5.67	2.10	4.51	2.66	5.55
$\Delta\psi$ (smooth approx.)	2.40	2.30	2.36	2.23	1.849	1.901	1.792	1.840	1.784	1.842
Average passage per proton	-	-	0.04	0.07	-	-	0.067	0.061	0.065	0.059
	16.9		16.0		9.2		10.8			

to formation of the halo in xx' phase space. The halo particles cause significant growth of the effective emittance and increase of the beam size in x-direction in a real space. This effect is clearly seen in fig.3 where the phase projections without and with space charge after the injection completion are shown.

In a working area there are strong coupling resonances $\nu_x = \nu_y$, $2\nu_y - \nu_x = 2$, $2\nu_x + 2\nu_y = 9$, $3\nu_x + \nu_y = 9$, $\nu_x + 3\nu_y = 9$. The coupling is caused by means of Coulomb field of the particles occupying the resonance band. So far as the beam space charge acts stronger in y-direction in the FEM the horizontal oscillation energy is transferred to the vertical motion for the resonance particles. This decreases the betatron oscillation amplitude in x-direction, increases the betatron oscillation amplitude in y-direction and therefore causes the reduction of $\epsilon_{x rms}$ and growth of $\epsilon_{y rms}$.

The distributions of stored particles over phase coordinates are shown in fig.4 after the injection completion at the stripping foil azimuth (the case without space charge is shaded).

On the whole, the beam parameters satisfy to the FEM of the storage ring operation and there are no additional difficulties with space charge in realization of such mode.

Slow extraction mode simulation

The characteristic functions of one half ring period for this mode are shown in fig.5. Beam parameters without and with space charge are shown in Table 1 after the injection completion and after 1000 turns. We assumed that a spiral injection is used only in vertical direction. The results display:

- the xx' -distribution is essentially nonhomogeneous, there is a great difference between $\epsilon_{x rms}$ and ϵ_x ;
- the space charge leads to decrease of $\epsilon_{y rms}$ (~20%) and increase of $\epsilon_{x rms}$;
- emittance ϵ_x grows by 1.5 times to the injection completion and by 1.9 times after 1000 turns.

It is necessary to mention that main changes of the beam parameters are finished to 400th turn. The betatron spectra are shown in fig.6 after the injection completion and after 1000 turns. In the resonance bands $4\nu_x = 7$ and $3\nu_x = 5$ there are 10% of the stored particles, moreover the main part of them occupies the periphery of the xx' emittance. These particles form a halo in the xx' phase space, cause the growth of effective emittance and beam size in x-direction in the real space. This effect is clearly seen in fig.7(a,b), where the xy and xx' projections of the beam phase volume are shown. The existence of the coupling resonances $\nu_x = \nu_y$, $2\nu_y - \nu_x = 2$, $2\nu_x + 2\nu_y = 7$, $3\nu_x + \nu_y = 7$

with essential difference between the energies of x- and y-motions leads to transfer of the vertical oscillation energy to the horizontal one for particles occupying the resonance bands. It means the betatron oscillation amplitude increases in x-direction and decreases in y-direction, therefore, $\epsilon_{x rms}$ grows and $\epsilon_{y rms}$ reduces, also additional halo particles are formed in xx' -plane.

Large energy difference of the vertical and horizontal motions leads to an intense energy transfer in this operation mode of the storage ring. The resonance band $2\nu_y - \nu_x = 2$ coincides well with the pit in ν_y -spectrum and the peak in ν_x -spectrum in fig.6 thus confirming the process mentioned above. The beam phase space $x'y'$ is shown in fig.7(c) after 1000 turns without and with space charge where the reduction of the vertical oscillation kinetic energy and growth of the horizontal oscillation kinetic energy is obvious. The distributions of particles over phase coordinates after the injection completion and after 1000 turns at the stripping foil azimuth are shown in fig.8 (the case with space charge is shaded).

The simulation has revealed the essential space charge influence on the stored beam parameters, mainly on the horizontal particle dynamics in the SEM of the storage ring operation. This must be taken into account in future to organize the stored beam extraction.

Conclusion

The results of simulation of the injection and circulation of high intensity beam in the INR proton storage ring have shown essential influence of space charge field nonlinearity on the stored beam parameters. This influence reveals itself in betatron spectrum formation and complex resonance interactions of the stored particles. Also the simulation results have shown that the main modes of the storage ring can be realized with satisfactory parameters of extracted beams.

References

- M.I.Grachev, et.al. Proc.XIII Int. Conf. on High Energy Accelerators, Novosibirsk, 1987, pp.264-269.
- V.A.Moiseev. INR preprint, P-540, Moscow, 1987.
- V.A.Moiseev. INR preprint, P-539, Moscow, 1987.
- A.Sorensen. Part. Accel., 6, 145, 1975.
- N.M.Kurbangaliev, et.al. Proc. All-Union Accelerators Conf., Dubna, 1987, p.246.

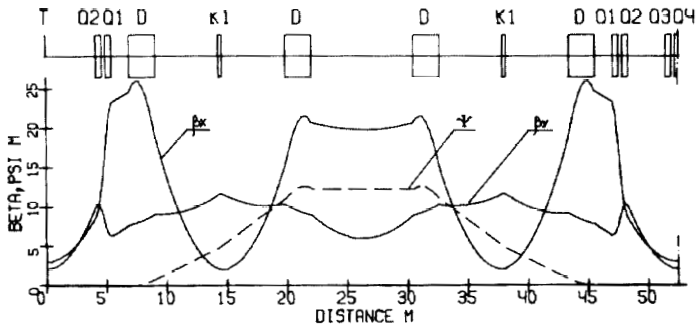


Fig. 1

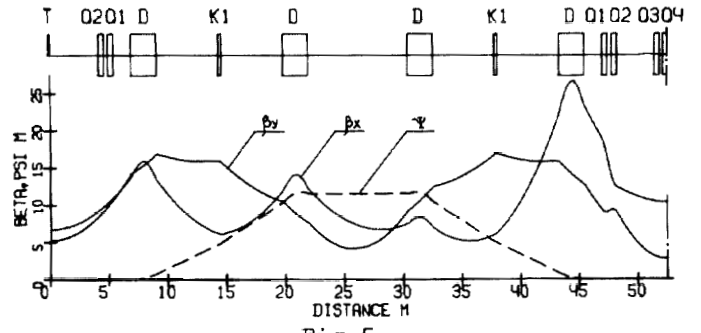


Fig. 5

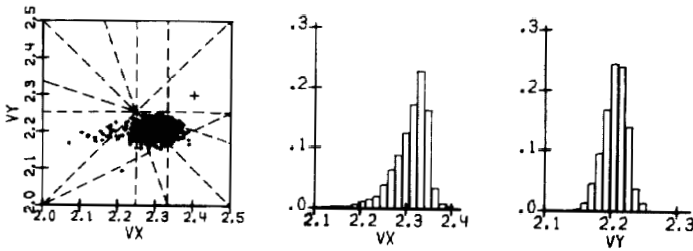


Fig. 2

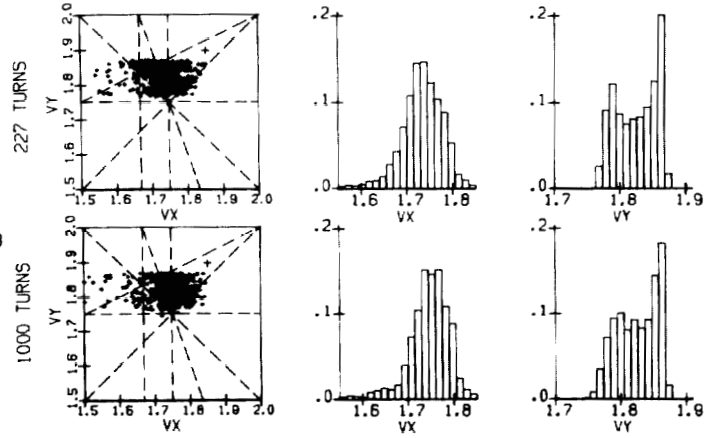


Fig. 6

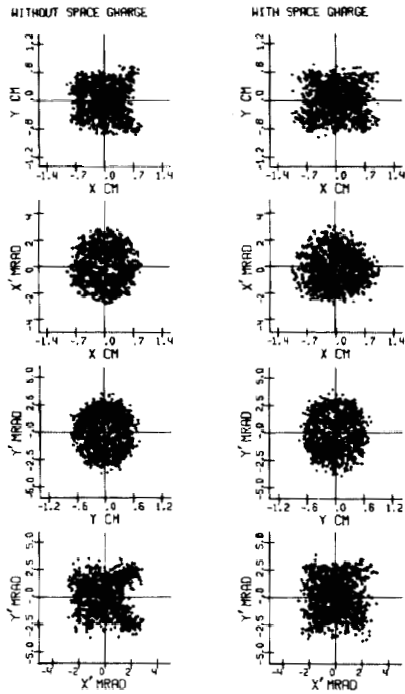


Fig. 3

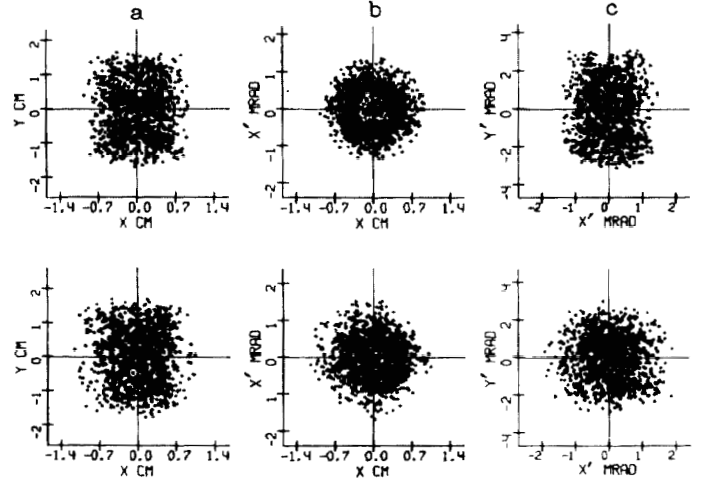


Fig. 7

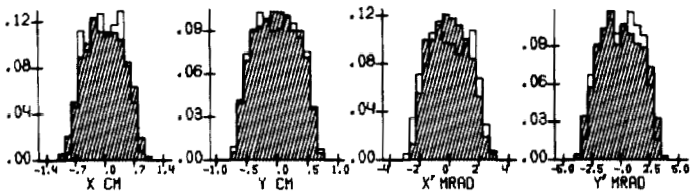


Fig. 4

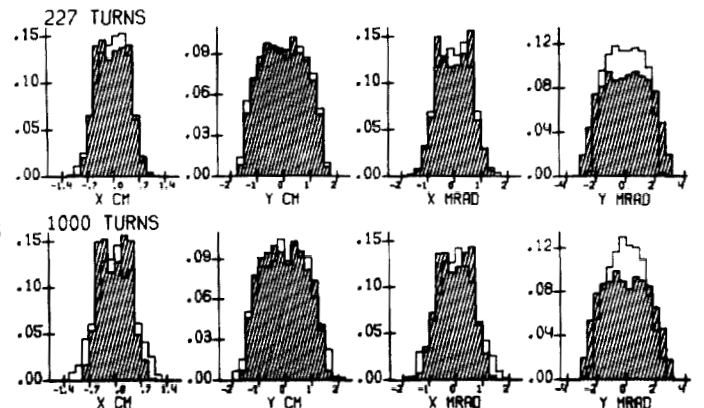


Fig. 8